Comparison of Neural Network Architectures for Simultaneous Tracking and Navigation with LEO Satellites

Sharbel E. Kozhaya †, Jamil A. Haidar-Ahmad†, Ali A. Abdallah†, Zaher M. Kassas†, and Samer S. Saab‡
† *University of California, Irvine, USA*
‡ *Lebanese American University, Byblos, Lebanon*

BIOGRAPHIES

Sharbel E. Kozhaya is a Ph.D student in the Department of Electrical Engineering and Computer Science at the University of California, Irvine and a member of the ASPIN Laboratory. He received a B.E. in Electrical Engineering from LAU. His current research interests include opportunistic navigation, software-defined radio, and low earth orbit satellites.

Jamil A. Haidar-Ahmad is a Ph.D student in the Department of Electrical Engineering and Computer Science at the University of California, Irvine and a member of the Autonomous Systems Perception, Intelligence, and Navigation (ASPIN) Laboratory. He received a B.E. in Mechatronics Engineering with honors and Minor in Computer Science from the Lebanese American University (LAU). His current research interests include opportunistic navigation, software-defined radio, signal fusion, 5G, and indoor localization.

Ali A. Abdallah is a Ph.D student in the Department of Electrical Engineering and Computer Science at the University of California, Irvine and a member of the ASPIN Laboratory. He received a B.E. in Electrical Engineering from LAU. His current research interests include opportunistic navigation, software-defined radio, long-term evolution (LTE), 5G, and indoor localization.

Zaher (Zak) M. Kassas is an associate professor at the University of California, Irvine and director of the Autonomous Systems Perception, Intelligence, and Navigation (ASPIN) Laboratory. He is also director of the U.S. Department of Transportation Center: CARMEN (Center for Automated Vehicle Research with Multimodal AssurEd Navigation), focusing on navigation resiliency and security of highly automated transportation systems. He received a B.E. in Electrical Engineering from the Lebanese American University, an M.S. in Electrical and Computer Engineering from The Ohio State University, and an M.S.E. in Aerospace Engineering and a Ph.D. in Electrical and Computer Engineering from The University of Texas at Austin. He is a recipient of the 2018 National Science Foundation (NSF) Faculty Early Career Development Program (CAREER) award, 2019 Office of Naval Research (ONR) Young Investigator Program (YIP) award, 2018 IEEE Walter Fried Award, 2018 Institute of Navigation (ION) Samuel Burka Award, and 2019 ION Col. Thomas Thurlow Award. His research interests include cyber-physical systems, estimation theory, navigation systems, autonomous vehicles, and intelligent transportation systems.

Samer S. Saab received the B.S., M.S., and Ph.D. degrees in electrical engineering in 1988, 1989, and 1992, respectively, and the M.A. degree in applied mathematics in 1990, from the University of Pittsburgh, PA, USA. He is currently the Dean of Graduate Studies and Research at the Lebanese American University. He served on the Editorial Board of the IEEE Transactions on Control Systems Technology from 2005 to 2011 and on the Editorial Board of the IEEE Control Systems Society-Conference from 2005 to 2009. Since September 2015, he has been serving on the Editorial Board of the IEEE Transactions on Automatic Control. His research interests include iterative learning control, Kalman filtering, navigational positioning systems, and wireless communications.

ABSTRACT

Machine learning (ML) frameworks are investigated for use in simultaneous tracking and navigation (STAN) with low Earth orbit (LEO) satellites. STAN is a navigation paradigm that utilizes specialized LEO receivers to extract navigation observables (e.g., pseudorange and Doppler) from LEO satellite signals. Two neural network architectures are compared: Feed Forward Neural Network (FFNN) and Recurrent Neural Network (RNN). Additionally, two ML-based orbit determination frameworks are compared: ephemeris propagation and residual error propagation. The

Preprint of the 2021 ION GNSS+ Conference St. Louis, Missouri, September 20–24, 2021

objective of the comparison is to select an approach with the lowest open-loop propagation error as well as computational cost. Based on simulation results, a nonlinear autoregressive neural network with exogenous inputs (NARX) embedded within the residual error modeling framework is selected as the best ML approach among the compared candidates. Experimental results are presented demonstrating a ground vehicle navigating for a total of 258 seconds, while receiving signals from two Orbcomm LEO satellites. Global navigation satellite system (GNSS) signals were artificially cut off for the last 30 seconds, during which the vehicle traversed a trajectory of 871 m. Two navigation frameworks are compared to estimate the vehicle's trajectory: (i) LEO signal-aided inertial navigation system (INS) STAN framework using Simplified General Perturbation (SGP4) as its propagator and (ii) the proposed LEO signal-aided INS STAN framework using ML as its propagator. The STAN with SGP4 achieved a three-dimensional (3-D) position root-mean squared error (RMSE) of 30 m. In contrast, the proposed STAN with SGP4+NARX framework achieved a 3-D position RMSE of 3.6 m.

I. INTRODUCTION

Over the past decades, the ambitious and glorified image of an Earth connected through a web weaved from low earth orbit (LEO) satellites had taken the world by storm, promising high-resolution images; remote sensing; space-based optical mesh networks; global, high-availability, high-bandwidth, and low-latency internet [1–3]. Many companies such as Globalstar, Iridium, ICO, and Teledesic made haste in securing their position in space as more constellations and satellite systems were born [4]. This dream was short-lived; however, as these companies suffered financial problems, and the reliability and viability of LEO constellations were scrutinized and suffered from skepticism. In the past decade, with the ground-breaking recent developments in satellite technologies and launch reduction costs, the world has set its sights on LEO satellites once again. The demand for LEO satellites has never been higher, as LEO satellites have the potential to serve as the foundation for supporting new technologies and advancements in satellite imaging, remote sensing, and revolutionizing communication technologies such as 5G which demands higher data rates [5–7]. Furthermore, the commercialization of LEO mega-constellations, LEO satellites' popularity has soared, with major technology giants such as SpaceX, Amazon, and Boeing rushing to enter this field by launching and scheduling the launch of tens of thousands of satellites for internet connectivity and communication purposes [8, 9].

Signals transmitted by the tens of thousands of LEO satellites that are about to orbit the earth could be utilized as signals of opportunity (SOPs) for navigation purposes. SOPs come in different forms and multiple sources ranging from terrestrial signals such as digital television, cellular, and AM/FM to extraterrestrial signals such as signals coming from LEO or Medium Earth Orbit (MEO) satellites [10]. When it comes to navigation, these SOPs are a very attractive source in environments where global navigation satellite systems (GNSS) are unavailable (e.g., under interference or jamming attacks), unusable (e.g., indoors), too weak (e.g., deep urban canyons or under dense canopy), or untrustworthy (e.g., under spoofing attacks). Utilizing different SOPs for navigation in GNSS-challenged environments has been studied for: (i) terrestrial signals [11–19] and (ii) LEO signals [20–27]. As megaconstellations of LEO satellites get launched, LEO satellites will provide virtually a blanket cover around the globe, bringing forth abundant signals diverse in frequency (allowing for spoofing detection) and in direction (yielding a low geometric dilution of precision). They will also provide significantly more powerful signals compared to GNSS satellites which reside in MEO.

Since most LEO constellations are not intended for navigation purposes, three challenges must be tackled to exploit their signals for navigation: (i) develop specialized receivers to extract navigation observables from their downlink signals [28–33], (ii) compensate for lack of tight synchronization of satellites' clocks [34, 35], and (iii) estimate the satellites' ephemerides [36, 37]. This paper focuses on the latter challenge.

Several orbital determination methods have been developed in the literature [38–41]. These methods differ in complexity and accuracy. Numerous dynamics models which estimate the state of LEO satellites (position and velocity), as well as these estimates' uncertainty, have been developed over the years [42, 43]. The state of a satellite can be parametrized by its Keplerian elements, also known as classical orbital elements (COE). These orbital elements, along with some other information about a satellite' states, can be found in two-line element sets (TLEs) which are publicly published on a daily basis by the North American Aerospace Defense Command (NORAD) [44].

One way to mathematically propagate a satellite's states given its position vector in an inertial reference frame is to solve a second order differential equation relating the satellite's position and acceleration. This is also known

as a Kepler orbit, which is an unperturbed orbit where for any values of the initial state vector, the Kepler orbit corresponding to the solution can be found. However, utilizing these elements in determining an orbit through unperturbed Keplerian orbital models numerically or analytically leads to highly inaccurate results as there are several sources of perturbing forces that cannot be ignored, e.g., atmospheric drag, the Earth's oblateness causing a non-uniform gravitational field, solar radiation pressure, and other sources of gravitational forces (e.g., the Sun and the Moon). Therefore, perturbed models (e.g., two-body J2 propagator which takes into consideration the previously mentioned perturbations) are typically utilized, where an extra term is added as process noise in an attempt to capture the overall perturbation in acceleration, including multiple sources of forces which could offset the satellite's ephemeris from following an unperturbed path.

Numerical methods, such as the two body, two body with J2 model, and the High-Precision Orbit Propagator (HPOP) are capable of producing highly accurate orbits; however, they require heavy computational loads to forecast the satellite orbit, rendering them unsuitable in real-time navigation systems. Meanwhile, their analytical counterparts, such as the Simplified General Perturbation (SGP4) [45], are computationally more efficient, allowing for real-time propagation at the cost of introducing larger satellite position errors. The currently available parameters from NORAD, such as values from TLE files, do not provide enough data for achieving a desirable state accuracy, where utilizing these elements for orbital determination with a standard SGP4 propagator could lead to errors in the order of several kilometers, which accumulate and drift over time. These errors are in reality greater due to the fact that the initial estimation of the satellite's position purely from the TLE file parameters could be off by as much as 2.5 km [46, 47]. Recent studies had shown that more accurate results can be achieved in LEO-based navigation by simultaneously tracking the satellite's states in a navigation filter, or what is referred to as simultaneous tracking and navigation (STAN) framework [21]. STAN simultaneously estimates the LEO satellites' states together with the navigator's states. The SGP4 propagator would be a candidate model for usage within the STAN framework. However, the SGP4 propagator not only inherits TLE errors, but it cannot be initialized using any *a priori* knowledge of the position and velocity of the satellite– this means it depends exclusively on TLE files, which are periodically updated every 24 hours.

In the past decade, there has been increased interest in utilizing the powerful capabilities of machine learning (ML) for providing an orbital propagation solution. In [48] and [49], distribution regression was used for orbital determination of objects in LEO and GEO space. Propagating LEO space debris orbits was studied through the use of support vector machines (SVMs) [50, 51], and LEO satellite orbital states were modeled using artificial neural networks (ANNs), SVMs, and gaussian processes (GPs).

A simulation study showed that ANNs possess high regression capabilities compared to SVMs and GPs [51, 52]. However, these results compared the performance of different ML methods against each other, not taking into consideration the high accuracy of standard numerical and analytical propagators. Time delayed neural networks (TDNNs) and long short-term memory (LSTM) neural networks have been studied in [53]. However, utilizing ML in full orbital determination, allowing to completely replace standard propagators, is yet to be achieved.

A promising preliminary study was conducted in [37], in which a TDNN was trained using the data from two Orbcomm LEO satellites, which broadcast their 3-D position, which are obtained from onboard GNSS receivers. The TDNN's output was used in the STAN framework.

This paper builds on the results of [37] and makes the following contributions:

- It conducts a comprehensive performance analysis between different ANN architectures for short and long-term satellite orbit prediction, namely TDNNs and LSTMs.
- It studies the performance of the numerical and analytical propagators powered by a ML approach to account for residual error correction.
- It assesses the validation and generalization of the proposed ML-based orbital propagator for different orbits.
- It demonstrates experimentally the performance of the proposed ML-based STAN framework in estimating a ground vehicle's position.

The remainder of the paper is organized as follows. Section II briefly explains ML-based orbital determination and provides background on what has been achieved in literature. Section III describes the proposed architectures and the improvements compared to previous approaches. Section IV presents a series of numerical experiments where the ML models are investigated and discussed. Finally, concluding remarks are given in Section V.

II. OVERVIEW OF THE PROPOSED SYSTEM

This section presents a high-level block diagram of the proposed system. The proposed system builds on the traditional STAN framework introduced in [21]. The performance of the EKF-STAN framework has been previously demonstrated in realistic simulation environments and experimentally on a ground vehicle and on an unmanned aerial vehicle (UAV), showing the potential of achieving meter-level-accurate navigation [21, 37].

The EKF-STAN framework utilizes specialized LEO receivers to extract navigation observables, such as ephemeris messages, if available; pseudorange; and Doppler measurements from the LEO satellite signals. Furthermore, a model-based LEO propagator, such as SGP4, is employed in estimating the LEO satellite's states (position and velocity). The EKF-ML-STAN framework instead replaces the model-based propagator with a ML-based propagator to achieve potentially more accurate propagated LEO states. The framework includes GNSS receivers, which produce a navigation solution from GNSS signals, when such signals are available and useable. Finally, an IMU which reports the vehicle's specific force, angular rate, and orientation, is embedded within an INS. The INS provides the vehicle's position state, which along with the LEO signals, propagated LEO states, GNSS signals, and clock models which compensate for timing bias and phase shifts, are fed into an Extended Kalman Filter (EKF). The employed EKF then simultaneously estimates the vehicle's states, tracks the LEO satellite's states, and estimates timing biases as well as the confidence of the estimated values. When GNSS signals are available, the framework uses these signals for navigating the vehicle and tracking the LEO satellites. Once the GNSS signals cut off, the ML model propagates the LEO satellite states within the STAN framework. Fig. 1 depicts the proposed EKF-ML-STAN framework.

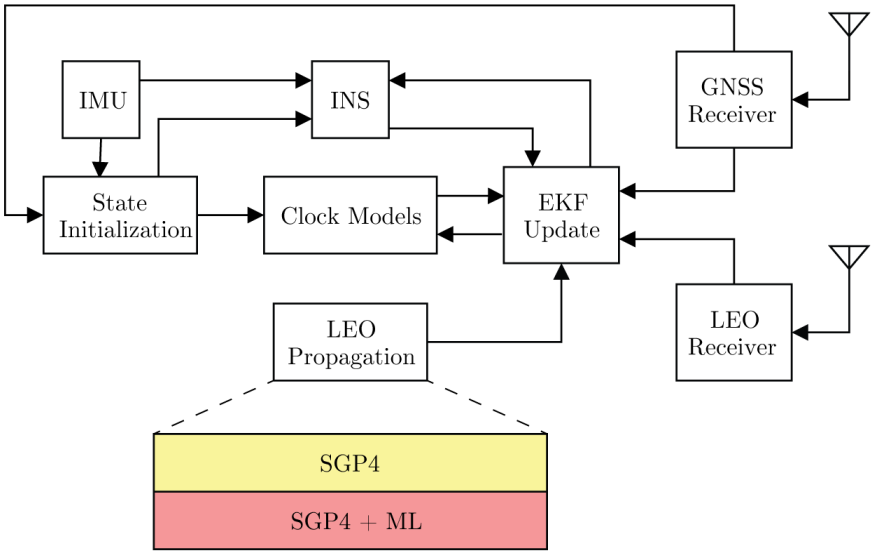

Fig. 1. Proposed improvements on the STAN system.

The proposed ML propagator approach could take one of two forms. The first form replaces the LEO propagation block with a specialized ML propagation block capable of directly estimating LEO satellite ephemeris. The second form adds an error correction block to the STAN framework right after the LEO propagation block. The error correction block learns the mapping between a standard propagator, such as SGP4, and a highly accurate propagator, such as HPOP.

III. ML-BASED ORBITAL DETERMINATION

ML attempts to build a model based on training data, which is subsequently utilized in several applications, such as making predictions or inferences, classifying data, or making decisions. ML has been utilized in solving highly dynamic, nonlinear, and highly uncertain problems. ML can be categorized into: (i) supervised learning, where the model is given both the input and expected output; (ii) unsupervised learning, where the model is only given the inputs; (iii) reinforced learning, where the model is given rewards or penalties according to the decisions it makes.

For orbital determination, a ML model would be given the task of taking previous LEO satellite positions as inputs and using this information to predict the satellite's future ephemeris. A complex ML model would be capable of embedding the highly dimensional dynamical orbital propagation models. The desired ML model should also propagate any initial *a priori* knowledge of a satellite's state. To this end, the model is expected to learn the behavior of highly accurate propagators, which would otherwise not be usable in real-time applications, such as HPOP. The model will serve as a substitute to highly accurate propagators with lower computational complexity, as inference times are usually low. The SGP4 propagator will be treated as the baseline for comparison with the proposed ML models. SGP4 is used to calculate orbital state vectors of satellites within an Earth-centered inertial (ECI) coordinate system. It is an analytical orbital propagator that uses TLE files, produced by NORAD and the National Aeronautics and Space Administration (NASA) daily. It is widely used in real-time orbital determination as it takes into consideration the perturbations a multitude of external forces. In order to compare the performance of the ML models with SGP4, a more accurate, yet computationally heavy propagator, HPOP, is considered as ground truth [54].

ANNs are systems capable of approximating any continuous function and are therefore known as "Universal Approximators" [55]. Consider some input $x \in \mathcal{X}$ that is mapped to $y \in \mathcal{Y}$ by an unknown function $f : \mathcal{X} \mapsto \mathcal{Y}$. Given enough compact subsets of data points mapping the input space and output space $\{(x_1, y_1), \ldots, (x_n, y_n)\}$, the neural network (NN) forms probability-weighted associations, effectively approximating the function that maps the two spaces. NNs are capable of achieving this by funneling the inputs through a multitude of "neuron" blocks, where every neuron computes $\sigma(x, w, b) = \sigma(w \cdot x + b)$, where w is the weight associated with every input, b is the bias associated with every input, and σ is the activation function of the neuron which could either be linear or could add nonlinearity to the system.

Once the estimated output $\hat{y}$, is computed, the error between the observed output y and $\hat{y}$ is calculated through a cost function $C(y, \hat{y})$, which the NN aims to minimize. There is an abundance of cost functions used in ML, each allowing for an intuitive understanding of the difference between the observed and estimated output. The mean-squared error (MSE) will be used as a cost function to assess the performance in the proposed approach, which can be expressed as

$$C(y, \hat{y})_{\text{MSE}} = \frac{1}{n} \sum_{i=1}^{n} (y_i - \hat{y}_i)^2 \tag{1}$$

where n is the number of data points, y_i is the observed values, and $\hat{y}_i$ is the estimated values. Once the cost function is computed, each layer's weights and biases are updated according to how much those weights and biases contributed to the each layer's error output.

To achieve a computationally feasible ML solution for orbital determination and propagation, this paper presents two frameworks: (i) ephemeris prediction and (ii) error prediction. First, the ephemeris propagation framework presents an architecture that is capable of propagating a satellite's orbit from historical state data, where each state is given by $S = [r, \dot{r}]^\intercal$, where r and $\dot{r}$ are the LEO satellite's 3-D position and velocity in the ECEF frame. There has been previous work in training a TDNN to model a satellite's path for a short time window (approximately 30 seconds) in [37]. However, this model used the LEO satellite's state which are transmitted by onboard GPS receiver and transmitted in the downlink signal. While this approach produced promising results with Orbcomm LEO satellites, this cannot be generalized to other LEO satellite constellations, since they do not necessarily transmit their states openly. As such, a more realistic approach would be to train the NN to model a computationally heavy yet highly accurate propagator, such as HPOP. This model would look at historical HPOP data during training, and then take d previous consecutive states to output the next state: $\hat{S}_t = \Lambda(\hat{S}_{t-1}, \hat{S}_{t-2}, \ldots, \hat{S}_{t-d})$, where Λ is the function that maps previous states to the next state. A key constraint to the complexity of this model in allowing higher dimensionality is the time needed for inference, as the model should stay within real-time timing constraints.

Second, the error propagation framework models the error between a fast and less accurate propagator, such as SPG4, with a more accurate propagator, such as HPOP. This method is attractive since both propagators already handle the computation of highly dynamic parameters, leaving the NN to simply "close the gap" between already two close propagators. The model is trained to find the mapping from SPG4 propagated state vectors to HPOP propagated state vectors $\hat{S}_{\text{HPOP}} = \Gamma(S_{\text{SGP4}})$, where Γ is the mapping between the two states.

A. FRAMEWORK 1: Ephemeris Propagation

This section presents a ML model specialized for predicting LEO satellite orbits for short time windows.

A.1 TRAINING

The proposed ANN models are investigated to study their ability and accuracy in predicting a LEO satellite's state vector (3-D position and velocity). Ground truth data in the ECEF reference frame was acquired using the Analytical Graphics Inc. System Tool Kit (AGI-STK) software, which is capable of generating highly accurate orbits through the usage of the HPOP, a numerical propagator with high dimensionality and high fidelity [56]. The AGI-STK allows for exporting such orbits for usage in a ML environment. The satellite chosen for the simulation study is the Orbcomm F107 satellite (NORAD ID: 40087). AGI-STK provides its own database of satellite models, where this satellite's model parameters, such as its inertial mass distribution, are available. The toolkit provides a HPOP propagator with updated force models from its database. The force models include gravitational effects of the sun, moon, and options to include Jupiter, Venus, Saturn, and other planetary gravitational forces. The gravitational effects include Earth's gravitational model (2008) with high order and degree. Other forces include drag models, taking into account area/mass ratio, atmospheric density models, low altitude density models, and solar flux/geomagnetic models. Additionally, solar radiation pressure is utilized by the propagator while taking into account central body radiation pressure and eclipsing central bodies of the Earth and Moon. This makes the AGI-STK tool suitable for exporting propagated LEO satellite ephemeris to be used for training, validation, and testing.

A.2 DESIGN

To achieve a ML model which could take initial historical data and start propagating the satellite's orbit, using its previous output as new input, this model should be capable of time series prediction, as the satellite's state elements could be seen as its own time series. Feed forward neural networks (FFNN) [57,58], which simply propagate from input to output in one direction. However, other NNs like recurrent NNs (RNNs), close the loop and provide a feedback to the NN. For this reason, the RNNs are expected to perform well in modeling highly nonlinear and harmonic data [59–62].

TDNNs are simple FFNNs, except that in TDNNs the input is fed as a time series, which allows the NN to learn the dynamics of the system. For orbital determination, the output $\hat{y}(t)$ is the state vector $S_{\text{LEO}}(t)$ at time t, and the input is $I(0,1,\ldots,N-1) = \{x(t), x(t-\tau), \ldots, x(t-(N-1)\tau)\}$ for N previous state vector data points. The TDNN's output is connected to the input I through a delay block, closing the loop, and effectively creating a nonlinear auto-regressive (NAR) prediction model. The TDNN model is given an initial input I_0, and it predicts the next state of the satellite which is fed back as the new input. Fig. 2 depicts the structure of TDNN.

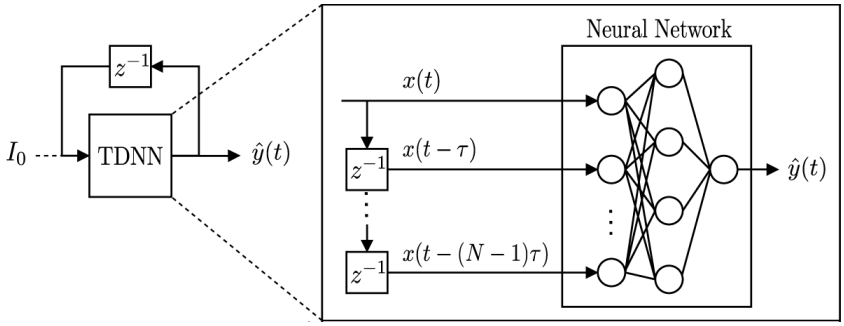

Fig. 2. TDNN architecture.

LSTMs are mainly composed of a cell which remembers values over time intervals (memory cell), an input gate, output gate, and a forget gate which regulates the flow of information into and out of the cell [63]. Fig. 3 presents the structure of LSTM NN.

The next subsection compares the performance of TDNN and LSTM for short orbital prediction.

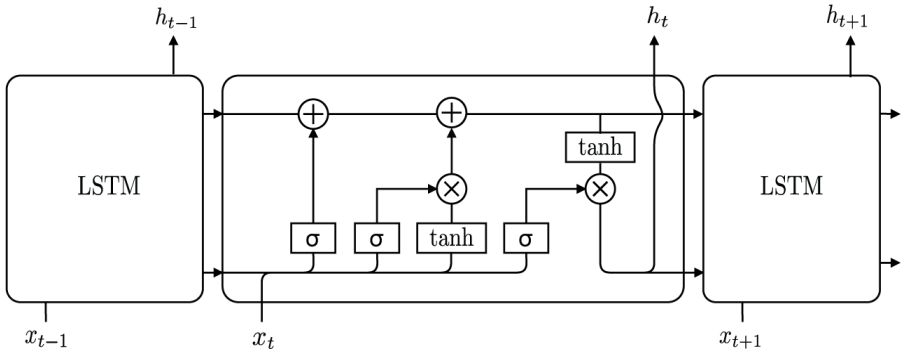

Fig. 3. Generic LSTM Architecture.

A.3 RESULTS

A simulation study was conducted using the data generated from the AGI-STK software corresponding to the an Orbcomm LEO satellite. Table I summarizes the simulation settings. Fig. 4 plots the training and validation MSEs as a function of training epochs. The validation errors for the TDNN design are low, showcasing its ability to function within an acceptable margin of error with new data. The LSTM is shown to be capable of following the profile of the LEO satellite's orbit, however, its accuracy was much lower.

TABLE I
SIMULATION SETTINGS.

Parameter	Value
Satellite name	Orbcomm F107
Duration [hours]	10
Sampling time [seconds]	1
Training Period [hours]	5
Testing Period [hours]	5

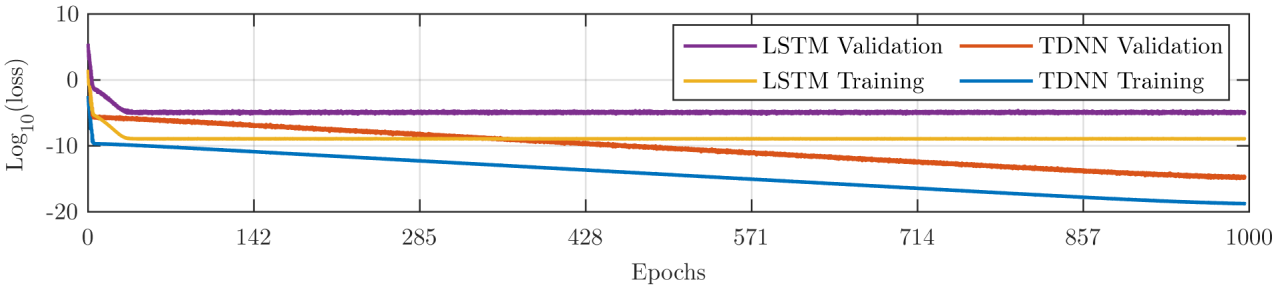

Fig. 4. Validation loss (MSE) versus number of training epochs of proposed models.

The training and validation errors show that the TDNN architecture outperforms the LSTM. The TDNN model is assessed by predicting the satellite's ephemeris in a closed-loop fashion. A TDNN model was trained for every output pair of parameters in the orbital state $S = \{x, y, z, vx, vy, vz\}$. The input and output were chosen as pairs of the position and velocity in each dimension at a time. Simulation results showed promising propagation accuracy for long-term windows, while using the proposed TDNN-based approach compared to the conventional SGP4 model. Fig. 5 depicts the error comparison of SPG4 and the TDNN corresponding to the $\{x, \dot{x}\}$ pair.

The results suggests that the TDNN model is capable of following the HPOP propagator for a short time window. The TDNN showed an acceptable performance for about one orbit, after which, the performance starts degrading.

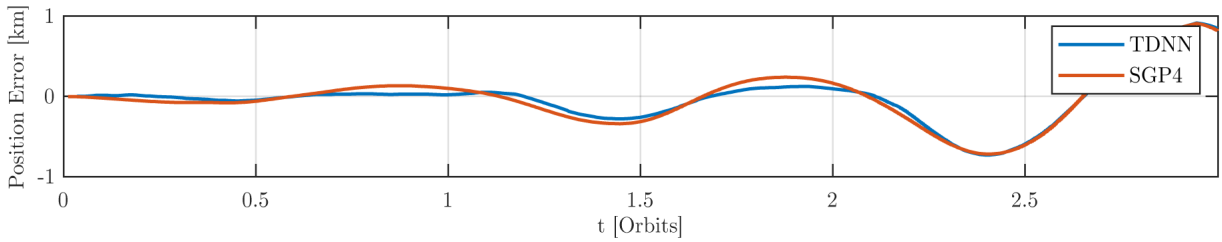

Fig. 5. LEO satellite's position error comparison between SGP4 and TDNN.

B. FRAMEWORK 2: Residual Error Propagation

The errors of the proposed ANNs with respect to HPOP were close to those of SGP4. This could be attributed to the complexity of the LEO satellite's orbit, as well as the highly dimensional properties of HPOP. SGP4 itself is accurate as well, though not as accurate as HPOP, in propagating the ephemeris. Therefore, a nonlinear autoregressive with exogenous inputs (NARX) model was devised to map the output of an SGP4 propagator to those of a well-initialized HPOP propagator.

B.1 TRAINING

To compare both proposed frameworks, the same training, validation, and testing data extracted from AGI-STK's HPOP propagated ephemeris are utilized.

B.2 DESIGN

The NARX model essentially functions similar to a NAR model, with the only difference being that exogenous inputs, which are propagated SPG4 ephemeris, are utilized in predicting the output, as seen in Fig. 6. The NARX architecture has been shown to be highly capable of learning long-term dependencies [64] and predicting time series [65–67]; even chaotic time series [68].

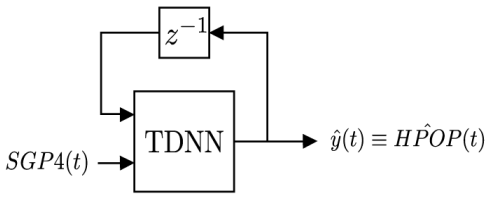

Fig. 6. Proposed NARX model.

The NARX architecture takes SGP4 propagated position states as inputs. It also has a feedback loop where its output, the estimated HPOP state values, are fed back as additional input. This way, the model takes SGP4 as input as well as previous estimated $\hat{\text{HPOP}}(t-1,\ldots,t-d)$ values, and it outputs new estimated $\hat{\text{HPOP}}(t)$ values.

B.3 RESULTS

The simulation settings shown in Table I for the Orbcomm LEO satellite were used. Fig. 7 and Table II shows the position error magnitude of the SGP4 versus the propagated SGP4+NARX approach. Because the SGP4 propagator is initialized with TLE files, which are a compact mean to achieve modestly fast and accurate calculation, its initial position error can reach up to 1 km [69]. Fig. 7 (a) shows the SGP4 position error magnitude while keeping the initial error. Fig. 7 (b) shows the SGP4 position error magnitude while removing the initial error of the TLE file for comparison. The results shows that SGP4+NARX is accumulating error at a much slower rate compared to SGP4.

From these results, one concludes that SGP4+NARX offers promising orbit propagation.

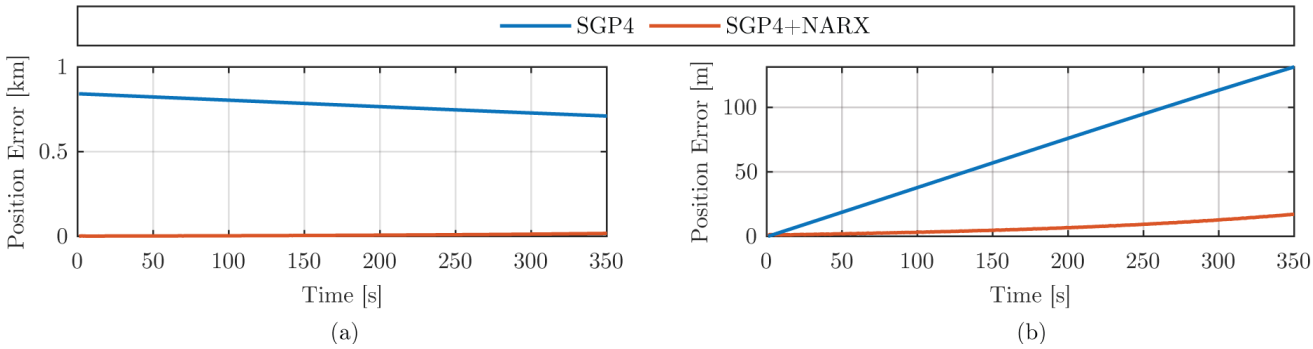

(a) (b)

Fig. 7. 3-D Position error magnitude for Orbcomm FM107's trajectory (a) without removing the initial error of SGP4 and (b) with removing the initial error of SGP4.

TABLE II
LEO PROPAGATION PERFORMANCE IN SIMULATION FOR 350 SECONDS.

RMSE [m]	**Orbcomm-FM107**
SGP4 (with TLE initial error)	773
SGP4 (without TLE initial error)	54
SGP4+NARX	8

IV. EXPERIMENTAL RESULTS

In this section, the performance of the proposed STAN navigation framework is assessed experimentally. Here, the performance utilizing propagation via SGP4 ill be compared to the one achieved with the proposed SGP4+NARX. In the experiment, Orbcomm LEO satellites signals were collected, where a ground-truth reference of the satellite ephemeris was obtained by decoding the satellites' positions transmitted from their on-board GPS receivers [28]. The error estimation NARX architecture was chosen, as it has demonstrated the highest accuracy amongst the studied ML frameworks.

A. ENVIRONMENTAL LAYOUT AND EXPERIMENTAL SETUP

A ground vehicle was equipped with the following hardware and software setup:

- A quadrifilar helix antenna to receive the Orbcomm SV downlink signals, which are transmitted at frequencies between 137 and 138 MHz
- A USRP E312 to sample Orbcomm symmetric differential phase shift keying (SDPSK) signals.
- These samples were then processed by the Multi-channel Adaptive TRansceiver Information eXtractor (MATRIX) software-defined radio developed by the Autonomous Systems Perception, Intelligence, and Navigation (ASPIN) Laboratory to perform carrier synchronization, extract pseudorange rate observables, and decode Orbcomm ephemeris messages [28].
- A Septentrio AsteRx-i V integrated GNSS-IMU, which is equipped with a dual-antenna, multi-frequency GNSS receiver and a Vectornav VN-100 micro-electromechanical system (MEMS) IMU. Septentrio's post-processing software development kit (PP-SDK) was used to process GPS carrier phase observables collected by the AsteRxi V and by a nearby differential GPS base station to obtain a carrier phase-based navigation solution. This integrated GNSS-IMU real-time kinematic (RTK) system [70] was used to produce the ground truth results with which the proposed navigation framework was compared.

The experimental setup is shown in Fig. 8. The ground vehicle was driven along U.S. Interstate 5 near Irvine, California, USA, for 7,495 m over 258 seconds, during which 2 Orbcomm LEO satellites were available. The standard deviation of the Orbcomm Doppler measurements was set to be 4.7 Hz, which was obtained empirically. Two navigation frameworks were implemented to estimate the vehicle's trajectory: (i) the LEO signal-aided INS STAN framework using SGP4 as its propagator and (ii) the LEO signal-aided INS STAN framework using the NARX as its

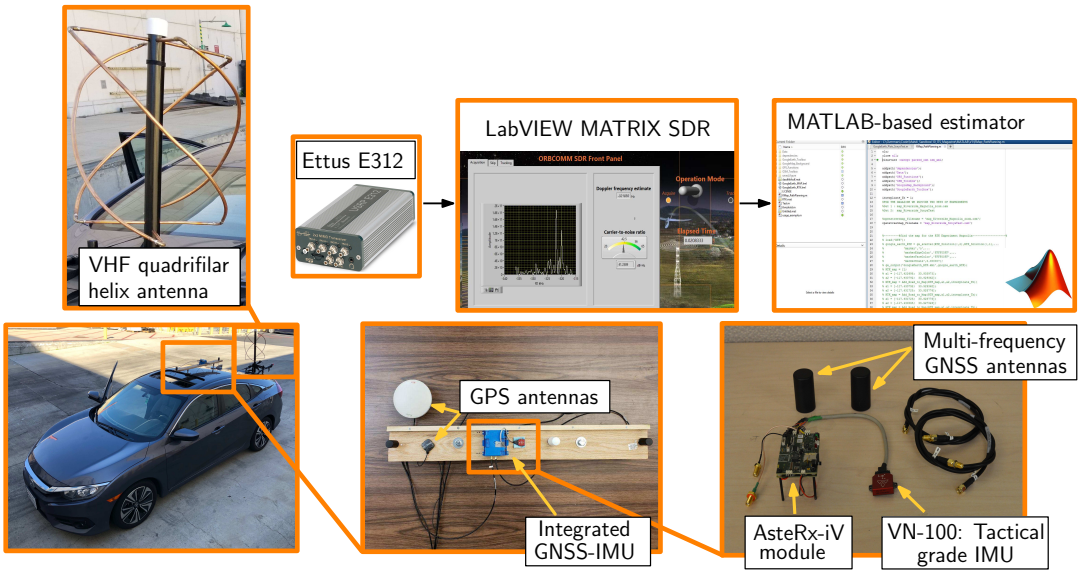

Fig. 8. Experimental Setup.

propagator. The SGP4 propagated ephemeris was initialized from the corresponding TLE file published by NORAD. The HPOP ephemeris utilized for training was properly initialized through STK, using the Orbcomm LEO satellite's positions decoded from the first measurement epoch. To perform a fair comparison between the propagation of SGP4+NARX that uses the first decoded ephemeris point for initialization and the performance of SGP4 that uses a relatively old TLE file, we generated a new TLE file the transmitted ephemeris, propagated it with SGP4, and used it for the comparison. Fig. 9 sketches the data generation and testing method.

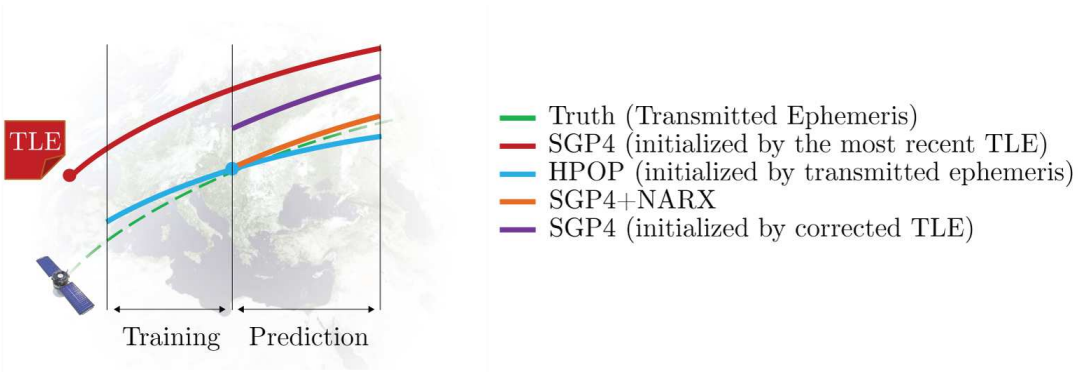

Fig. 9. Sketch illustrating the training phase of the NARX model (using TLE-SGP4 and HPOP) as its prediction phase.

B. RESULTS

First, the performance of the SGP4+NARX model as a propagator is compared with SGP4. The ephemeris position error $E_{\text{LEO}} = \{E_x, E_y, E_z\}$ of both tracked satellites and the total positional error characterized by $E_r = \sqrt{E_x^2 + E_y^2 + E_z^2}$ are shown in Fig. 10 and summarized in Table III.

The improved results in LEO satellite position estimation translate directly to a better navigation performance for a ground vehicle. Fig. 11 shows the vehicle's true trajectory compared to estimates from the original STAN framework and the proposed STAN with SGP4+NARX. The results are summarized in Table IV. The results show how the NARX model's ability in better estimating the LEO satellites' ephemeris leads to a more accurate navigation solution.

TABLE III
LEO Propagation Performance in an experimental scenario.

RMSE [m]	Orbcomm FM112	Orbcomm FM117
SGP4	558	1,226
SGP4+NARX	74	38

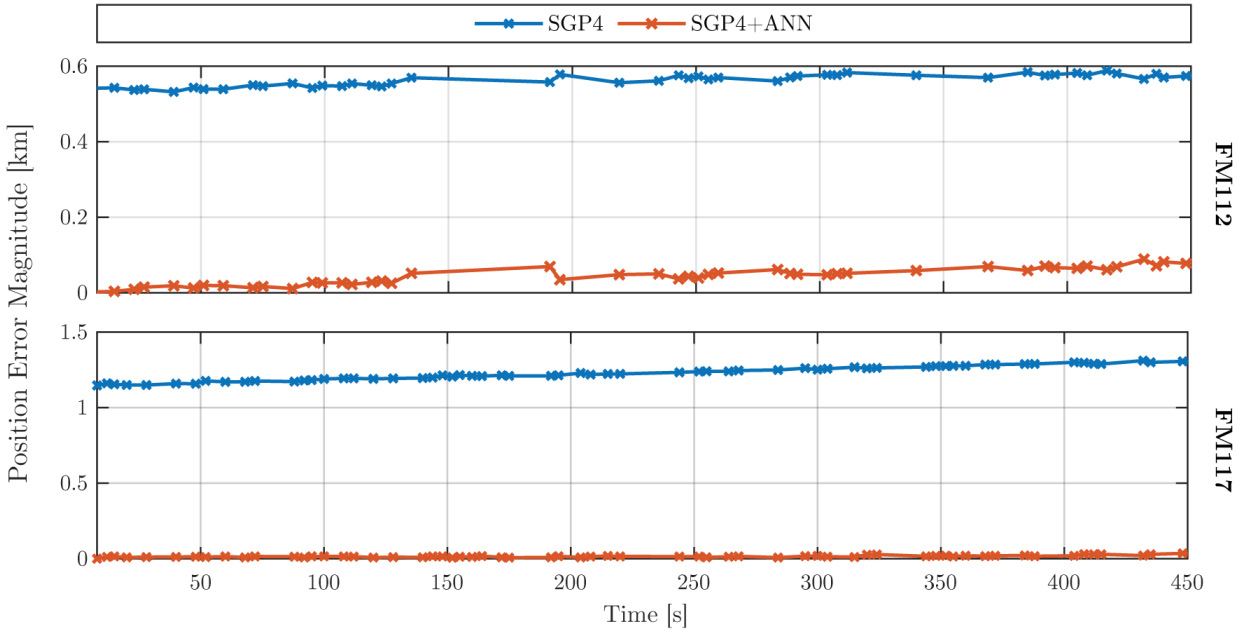

Fig. 10. Comparison between SGP4 and SGP4+NARX propagation

V. CONCLUSION

This paper investigated the performance of multiple ML models (TDNN, LSTM, NAR, and NARX) in propagating LEO satellite ephemeris and in correcting SGP4 ephemeris to map to a more accurate HPOP ephemeris. Both the ephemeris propagation framework and the error modeling framework were studied under the same simulation environment. The error modeling framework performed better and was thus chosen as the LEO propagator in the STAN framework. Experiments were conducted with a ground vehicle navigating while extracting Doppler measurements from two Orbcomm LEO satellites. The training data for the ML model was historical HPOP ephemeris data of the satellite's orbit. The performance of the SGP4+NARX model in tracking the LEO satellites' ephemeris was compared with the results of a traditional LEO propagation model using SPG4. The EKF with SGP4+NARX framework noticeably outperformed the traditional EKF with SGP4 framework's accuracy. The STAN with SGP4 achieved a ground vehicle 3-D position RMSE of 30 m. In contrast, the proposed STAN with SGP4+NARX framework achieved a 3-D position RMSE of 3.6 m.

ACKNOWLEDGMENT

This work was supported in part by the Office of Naval Research (ONR) under Grant N00014-19-1-2511 and Grant N00014-19-1-2613, and in part by the U.S. Department of Transportation (USDOT) under Grant 69A3552047138 for the CARMEN University Transportation Center (UTC). The authors would like to thank Analytical Graphics, Inc. (AGI) for making Systems Tool Kit (STK) available for research purposes.

TABLE IV
GROUND VEHICLE NAVIGATION PERFORMANCE.

Performance Measure	STAN with SGP4	STAN with SGP4+NARX
RMSE [m]	30	3.6
Final Error [m]	30	8.3

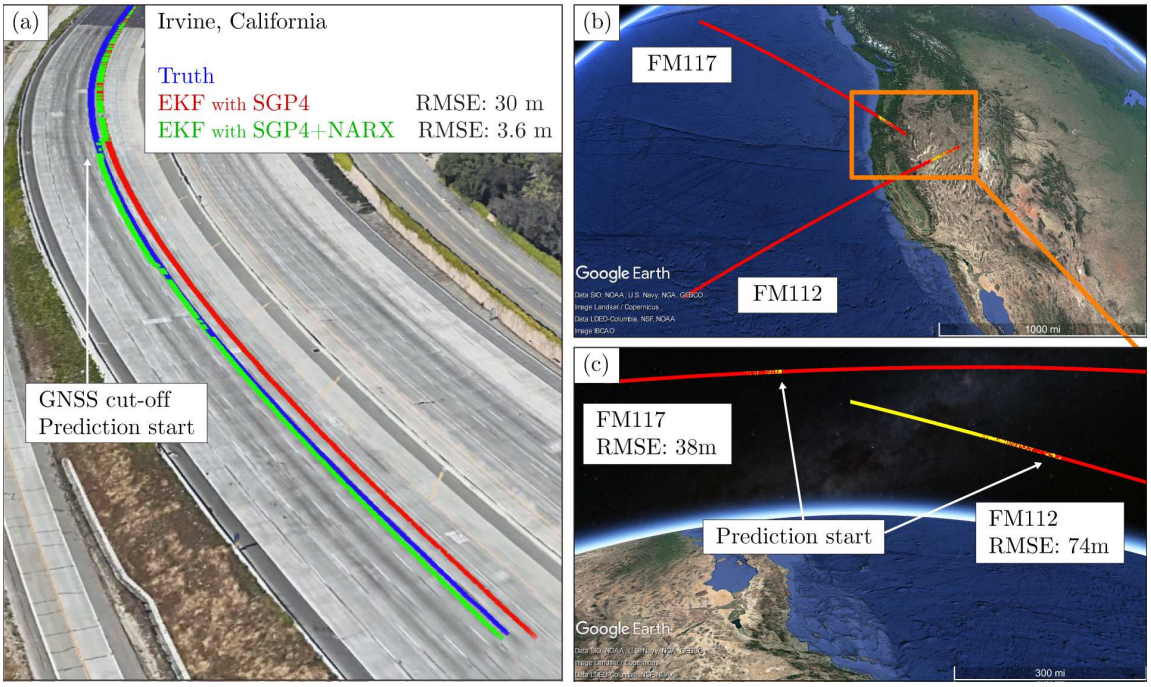

Fig. 11. Experimental results showing (a) the trajectory of a ground vehicle navigating with the proposed approach. The truth (white) is compared to the STAN with SGP4 estimate (red) and the STAN with SGP4+NARX estimate (green). (b, c) the trajectory of the 2 Orbcomm LEO satellites generated by SGP4+NARX predictions (yellow) versus the truth trajectories (red) obtained from onboard GPS receivers. Map data: Google Earth.

References

[1] S. Hackel, O. Montenbruck, P. Steigenberger, U. Balss, C. Gisinger, and M. Eineder, "Model improvements and validation of TerraSAR-X precise orbit determination," *Journal of Geodesy*, vol. 91, no. 5, pp. 547–562, 2017.

[2] D. King, A. Farrel, and Z. Chen, "An evolution of optical network control: From earth to space," in *Proceedings of the IEEE International Conference on Transparent Optical Networks*, 2020, pp. 1–4.

[3] D. Cho, W. Choi, M. Kim, J. Kim, E. Sim, and H. Kim, "High-resolution image and video CubeSat (HiREV): development of space technology test platform using a low-cost CubeSat platform," *International Journal of Aerospace Engineering*, 2019.

[4] D. Crosbie, "The new space race: Satellite mobile communications," *IEE review*, vol. 39, no. 3, pp. 111–114, 1993.

[5] O. Kodheli, A. Guidotti, and A. Vanelli-Coralli, "Integration of satellites in 5G through LEO constellations," in *Proceedings of the IEEE Global Communications Conference*, 2018, pp. 1–6.

[6] G. Giambene, S. Kota, and P. Pillai, "Satellite-5G integration: A network perspective," *IEEE Network*, vol. 32, no. 5, pp. 25–31, 2018.

[7] B. Di, L. Song, Y. Li, and V. Poor, "Ultra-dense LEO: Integration of satellite access networks into 5G and beyond," *IEEE Wireless Communications*, vol. 26, no. 2, pp. 62–69, 2019.

[8] D. Bhattacherjee, W. Aqeel, I. Bozkurt, A. Aguirre, B. Chandrasekaran, P. Godfrey, G. Laughlin, B. Maggs, and A. Singla, "Gearing up for the 21st century space race," in *Proceedings of the ACM Workshop on Hot Topics in Networks*, 2018, pp. 113–119.

[9] M. Harris, "Tech giants race to build orbital internet [news]," *IEEE Spectrum*, vol. 55, no. 6, pp. 10–11, 2018.

[10] "Position, navigation, and timing technologies in the 21st century," J. Morton, F. van Diggelen, J. Spilker, Jr., and B. Parkinson, Eds. Wiley-IEEE, 2021, vol. 2, Part D: Position, Navigation, and Timing Using Radio Signals-of-Opportunity, ch. 35–43, pp. 1115–1412.

[11] A. Popleteev, "Indoor positioning using FM radio signals," Ph.D. dissertation, University of Trento, Italy, 2011.

[12] C. Gentner, "Channel-SLAM: Multipath assisted positioning," Ph.D. dissertation, Ulm University, 2018.

[13] A. Shahmansoori, G. Garcia, G. Destino, G. Seco-Granados, and H. Wymeersch, "Position and orientation estimation through millimeter-wave MIMO in 5G systems," *IEEE Transactions on Wireless Communications*, vol. 17, no. 3, March 2018.

[14] J. Khalife and Z. Kassas, "Opportunistic UAV navigation with carrier phase measurements from asynchronous cellular signals," *IEEE Transactions on Aerospace and Electronic Systems*, vol. 56, no. 4, pp. 3285–3301, August 2020.

[15] C. Yang and A. Soloviev, "Mobile positioning with signals of opportunity in urban and urban canyon environments," in *IEEE/ION Position, Location, and Navigation Symposium*, April 2020, pp. 1043–1059.

[16] Z. Kassas, J. Khalife, A. Abdallah, and C. Lee, "I am not afraid of the jammer: navigating with signals of opportunity in GPS-denied environments," in *Proceedings of ION GNSS Conference*, 2020, pp. 1566–1585.

[17] Z. Kassas, A. Abdallah, and M. Orabi, "Carpe signum: seize the signal – opportunistic navigation with 5G," *Inside GNSS Magazine*, vol. 16, no. 1, pp. 52–57, 2021.

[18] T. Kazaz, G. Janssen, J. Romme, and A. Van der Veen, "Delay estimation for ranging and localization using multiband channel state information," *IEEE Transactions on Wireless Communications*, pp. 1–16, September 2021.

[19] A. Abdallah and Z. Kassas, "UAV navigation with 5G carrier phase measurements," in *Proceedings of ION GNSS Conference*, September 2021, accepted.

[20] D. Lawrence, H. Cobb, G. Gutt, M. OConnor, T. Reid, T. Walter, and D. Whelan, "Navigation from LEO: Current capability and future promise," *GPS World Magazine*, vol. 28, no. 7, pp. 42–48, July 2017.

[21] Z. Kassas, J. Morales, and J. Khalife, "New-age satellite-based navigation – STAN: simultaneous tracking and navigation with LEO satellite signals," *Inside GNSS Magazine*, vol. 14, no. 4, pp. 56–65, 2019.

[22] T. Reid, K. Gunning, A. Perkins, S. Lo, and T. Walter, "Going back for the future: Large/mega LEO constellations for navigation," in *Proceedings of ION GNSS Conference*, September 2019, pp. 2452–2468.

[23] Z. Kassas, J. Khalife, M. Neinavaie, and T. Mortlock, "Opportunity comes knocking: overcoming GPS vulnerabilities with other satellites' signals," *Inside Unmanned Systems Magazine*, pp. 30–35, June/July 2020.

[24] F. Farhangian, H. Benzerrouk, and R. Landry, "Opportunistic in-flight INS alignment using LEO satellites and a rotatory IMU platform," *Aerospace*, vol. 8, no. 10, pp. 280–281, 2021.

[25] S. Thompson, S. Martin, and D. Bevly, "Single differenced doppler positioning with low Earth orbit signals of opportunity and angle of arrival estimation," in *Proceedings of ION International Technical Meeting*, 2020, pp. 497–509.

[26] M. Psiaki, "Navigation using carrier doppler shift from a LEO constellation: TRANSIT on steroids," *NAVIGATION, Journal of the Institute of Navigation*, vol. 68, no. 3, pp. 621–641, September 2021.

[27] M. Neinavaie, J. Khalife, and Z. Kassas, "Exploiting Starlink signals for navigation: first results," in *Proceedings of ION GNSS Conference*, September 2021, accepted.

[28] J. Khalife and Z. Kassas, "Receiver design for Doppler positioning with LEO satellites," in *Proceedings of IEEE International Conference on Acoustics, Speech and Signal Processing*, May 2019, pp. 5506–5510.

[29] R. Landry, A. Nguyen, H. Rasaee, A. Amrhar, X. Fang, and H. Benzerrouk, "Iridium Next LEO satellites as an alternative PNT in GNSS denied environments–part 1," *Inside GNSS Magazine*, vol. 14, no. 3, pp. 56–64., May 2019.

[30] Z. Tan, H. Qin, L. Cong, and C. Zhao, "New method for positioning using IRIDIUM satellite signals of opportunity," *IEEE Access*, vol. 7, pp. 83 412–83 423, 2019.

[31] M. Neinavaie, J. Khalife, and Z. Kassas, "Blind Doppler tracking and beacon detection for opportunistic navigation with LEO satellite signals," in *Proceedings of IEEE Aerospace Conference*, March 2021, pp. 1–8.

[32] J. Khalife, M. Neinavaie, and Z. Kassas, "Blind Doppler tracking from OFDM signals transmitted by broadband LEO satellites," in *Proceedings of IEEE Vehicular Technology Conference*, April 2021, pp. 1–6.

[33] J. Khalife, M. Neinavaie, and Z. Kassas, "The first carrier phase tracking and positioning results with Starlink LEO satellite signals," *IEEE Transactions on Aerospace and Electronic Systems*, 2021, accepted.

[34] J. Khalife, M. Neinavaie, and Z. Kassas, "Navigation with differential carrier phase measurements from megaconstellation LEO satellites," in *Proceedings of IEEE/ION Position, Location, and Navigation Symposium*, April 2020, pp. 1393–1404.

[35] T. Mortlock and Z. Kassas, "Performance analysis of simultaneous tracking and navigation with LEO satellites," in *Proceedings of ION GNSS Conference*, September 2020, pp. 2416–2429.

[36] J. Morales, J. Khalife, U. Santa Cruz, and Z. Kassas, "Orbit modeling for simultaneous tracking and navigation using LEO satellite signals," in *Proceedings of ION GNSS Conference*, September 2019, pp. 2090–2099.

[37] T. Mortlock and Z. Kassas, "Assessing machine learning for LEO satellite orbit determination in simultaneous tracking and navigation," in *Proceedings of IEEE Aerospace Conference*, March 2021, pp. 1–8.

[38] X. Bai and J. Junkins, "Modified chebyshev-picard iteration methods for orbit propagation," *The Journal of the Astronautical Sciences*, vol. 58, no. 4, pp. 583–613, 2011.

[39] J. Aristoff and A. Poore, "Implicit runge-kutta methods for orbit propagation," in *AIAA/AAS Astrodynamics Specialist Conference*, 2012, p. 4880.

[40] J. Sullivan, S. Grimberg, and S. DAmico, "Comprehensive survey and assessment of spacecraft relative motion dynamics models," *Journal of Guidance, Control, and Dynamics*, vol. 40, no. 8, pp. 1837–1859, 2017.

[41] S. Shuster, *A survey and performance analysis of orbit propagators for LEO, GEO, and highly elliptical orbits.* Utah State University, 2017.

[42] X. Tian, G. Chen, E. Blasch, K. Pham, and Y. Bar-Shalom, "Comparison of three approximate kinematic models for space object tracking," in *Proceedings of International Conference on Information Fusion*, 2013, pp. 1005–1012.

[43] Y. Luo and Z. Yang, "A review of uncertainty propagation in orbital mechanics," *Progress in Aerospace Sciences*, vol. 89, pp. 23–39, February 2017.

[44] North American Aerospace Defense Command (NORAD), "Two-line element sets," http://celestrak.com/NORAD/elements/.

[45] D. Vallado, P. Crawford, R. Hujsak, and T. Kelso, "Revisiting spacetrack report# 3," in *Proceedings of the Astrodynamics Specialist Conference and Exhibit*, 2006, p. 6753.

[46] M. Zaheer, "Kinematic orbit determination of low earth orbiting satellites, using satellite-to-satellite tracking data and comparison of results with different propagators," 2014.

[47] D. Racelis and M. Joerger, "High-integrity TLE error models for MEO and GEO satellites," in *Proceedings of AIAA SPACE and Astronautics Forum and Exposition*, September 2018, pp. 1–13.

[48] S. Sharma and J. Cutler, "Robust orbit determination and classification: A learning theoretic approach," *IPN Progress Report*, pp. 42–203, 2015.

[49] F. Feng, Y. Zhang, H. Li, Y. Fang, Q. Huang, and X. Tao, "A novel space-based orbit determination method based on distribution regression and its sparse solution," *IEEE Access*, vol. 7, pp. 133 203–133 217, 2019.

[50] H. Peng and X. Bai, "Limits of machine learning approach on improving orbit prediction accuracy using support vector machine," in *Proceedings of the Advanced Maui Optical and Space Surveillance*, 2017, pp. 1–22.

[51] H. Peng and X. Bai, "Artificial neural network–based machine learning approach to improve orbit prediction accuracy," *Journal of Spacecraft and Rockets*, vol. 55, no. 5, pp. 1248–1260, 2018.

[52] H. Peng and X. Bai, "Comparative evaluation of three machine learning algorithms on improving orbit prediction accuracy," *Astrodynamics*, vol. 3, no. 4, pp. 325–343, 2019.

[53] N. Salleh, S. Yuhaniz, N. Azmi, and S. Sabri, "Enhancing simplified general perturbations-4 model for orbit propagation using deep learning: a review," in *Proceedings of the International Conference on Software and Computer Applications*, 2019, 5937–5941.

[54] C. Chao, J. Cook, J. Cox, T. Starchville, R. Thompson, and L. Wagner, "Independent verification and validation for analytical graphics, inc. of three astrodynamic functions of the satellite tool kit: version 4.1. 0," *Journal of The Aerospace Corporation ATR*, 2000.

[55] K. Hornik, M. Stinchcombe, and H. White, "Multilayer feedforward networks are universal approximators," *Neural networks*, vol. 2, no. 5, pp. 359–366, 1989.

[56] Analytical graphics, inc., systems tool kit (STK).

[57] M. Refan and A. Dameshghi, "GDOP classification and approximation by implementation of time delay neural network method for low-cost GPS receivers," *Iranian Journal of Electrical and Electronic Engineering*, vol. 16, no. 2, pp. 192–200, 2020.

[58] V. Peddinti, D. Povey, and S. Khudanpur, "A time delay neural network architecture for efficient modeling of long temporal contexts," in *Proceedings of the International Speech Communication Association Conference*, 2015.

[59] X. Yang, H. Sun, X. Sun, M. Yan, Z. Guo, and K. Fu, "Position detection and direction prediction for arbitrary-oriented ships via multitask rotation region convolutional neural network," *IEEE Access*, vol. 6, pp. 50 839–50 849, 2018.

[60] H. Kim and T. Bae, "Deep learning-based GNSS network-based real-time kinematic improvement for autonomous ground vehicle navigation," *Journal of Sensors*, 2019.

[61] M. Jiménez-Guarneros, P. Gómez-Gil, R. Fonseca-Delgado, M. Ramírez-Cortés, and V. Alarcón-Aquino, "Long-term prediction of a sine function using a LSTM neural network," *Journal of Nature-Inspired Design of Hybrid Intelligent Systems*, pp. 159–173, 2017.

[62] A. Hatata and M. Eladawy, "Prediction of the true harmonic current contribution of nonlinear loads using NARX neural network," *Alexandria Engineering Journal*, vol. 57, no. 3, pp. 2018–1518, 2007.

[63] F. Gers, J. Schmidhuber, and F. Cummins, "Learning to forget: Continual prediction with LSTM," *Neural computation*, vol. 12, no. 10, pp. 2451–2471, 2000.

[64] T. Lin, B. Horne, P. Tino, and C. Giles, "Learning long-term dependencies in NARX recurrent neural networks," *IEEE Transactions on Neural Networks*, vol. 7, no. 6, pp. 1329–1338, 1996.

[65] H. Siegelmann, B. Horne, and C. Giles, "Computational capabilities of recurrent NARX neural networks," *IEEE Transactions on Systems, Man, and Cybernetics, Part B (Cybernetics)*, vol. 27, no. 2, pp. 208–215, 1997.

[66] H. Xie, H. Tang, and Y. Liao, "Time series prediction based on NARX neural networks: An advanced approach," in *Proceedings of IEEE International conference on machine learning and cybernetics*, vol. 3, 2009, pp. 1275–1279.

[67] J. Menezes, P. Maria, and G. Barreto, "Long-term time series prediction with the NARX network: An empirical evaluation," *Neurocomputing*, vol. 71, no. 16-18, pp. 3335–3343, 2008.

[68] E. Diaconescu, "The use of NARX neural networks to predict chaotic time series," *Wseas Transactions on computer research*, vol. 3, no. 3, pp. 182–191, 2008.

[69] B. Li, J. Sang, and J. Ning, "TLE generation from sparse tracking data and its performance," *Advances in the Astronautical Sciences*, vol. 158, pp. 4003–4014, 2016.

[70] "Septentrio AsteRx-i V," https://www.septentrio.com/products, 2018.